Nuclear Instruments and Methods in Physics Research B 96 (1995) 619–625

NIM B
Beam Interactions with Materials & Atoms

ELSEVIER

Nonlinear screening and stopping powers at finite projectile velocities

E. Zaremba [a,*], A. Arnau [b], P.M. Echenique [b]

[a] *Department of Physics, Queen's University, Kingston, Ontario K7L 3N6, Canada*
[b] *Departamento de Física de Materiales, Universidad del País Vasco, San Sebastian, Spain*

Abstract

We have studied the nonlinear screening and stopping power of charged projectiles moving through a uniform electron gas with velocities up to the Fermi velocity of the gas. Our approach is based on density functional theory and is an extension of previous calculations which consider the screening of the projectile in the zero velocity limit. At the higher velocities considered here, the electrons of the metal occupy a shifted Fermi sphere which leads to an asymmetry of the screening charge density and scattering potential along the line of motion of the projectile. To obtain an approximate self-consistent solution of this dynamic screening problem, we use the spherically averaged density to define an averaged scattering potential (spherical potential approximation). As a specific application, we determine the axial screening charge density and stopping power of antiprotons in an electron gas characteristic of aluminium. Screening nonlinearities are found to be important for the full range of velocities considered. In addition, we find that the stopping power exhibits a linear dependence on velocity up to velocities approaching the stopping power maximum.

1. Introduction

The dynamic screening charge induced by the passage of a charged particle through matter is a central quantity required for an understanding of the electronic stopping power and other projectile–target interaction phenomena. The retarding force experienced by the projectile arises directly from the asymmetry of the induced charge density, and it is therefore of interest to determine how this asymmetry develops with increasing projectile velocity. For example, at high velocities the collective response of the medium becomes important and results in the formation of a trailing wake [1]. This influence of the projectile on the surrounding medium is most easily visualized in terms of the induced screening charge density and its associated electrostatic potential.

One approach commonly used to understand this behaviour is based on linear response theory as applied to the model of a uniform electron gas [1,2]. Although this dielectric function formalism provides a qualitative description of dynamic screening over the full range of projectile velocities, it is not quantitatively accurate. It is now well-known that a charged projectile represents a strong perturbation at low velocities and a description which goes beyond lowest order perturbation theory is needed to make contact with experimental stopping power measurements [3].

In going beyond linear response theory, several approaches are available, each with its own limitations. A particularly simple and appealing approach is a hydrodynamic description [4] in which the electron gas is treated as a charged fluid interacting with the moving external charge. The relevant dynamical variables are the electronic charge density and fluid velocity which together satisfy a set of coupled partial differential equations. Although essentially a classical picture, some quantum mechanical aspects can be included by using an equation of state obtained at the level of the Thomas–Fermi or Thomas–Fermi–von Weizsäcker approximation [5]. Contact with the linear response dielectric formalism is achieved by linearizing the hydrodynamic equations. However, the method is not restricted to the linear regime and a more accurate description is in principle available through a direct numerical solution of the full set of nonlinear equations. Some preliminary work [6] along these lines has demonstrated that this hydrodynamic approach is a useful complement to the more rigorous quantum mechanical methods.

A quite different extension of linear response theory is based on a systematic expansion in powers of the projectile charge Z. Within a many-body theory context, the induced density to second order in Z is determined by the so-called quadratic density response function which can be calculated within the random phase approximation. This is the same approximation used in the linear theory, and essentially constitutes a mean field theory of the electronic interactions. With this one approximation, the Z^3 correction to the stopping power was obtained in both the low [7]

* Corresponding author.

SSDI 0168-583X(95)00250-2

and high [8] velocity limits. More recently, the theory was extended to the full range of velocities spanning the stopping power maximum [9] and to date, represents the most complete description of the nonlinear corrections. However, being an expansion in Z, the theory is limited to those situations in which the corrections to the linear results are relatively small. In practice, for low projectile velocities this limits the theory to the lowest possible value of Z ($Z = 1$) and high electron densities. At velocities above the stopping power maximum, the Z^3 correction to the stopping power decreases more rapidly with velocity than the Z^2 contribution. As a result, nonlinear effects become relatively less important and the quadratic response theory can be used to obtain a good qualitative understanding of nonlinearities in the high velocity regime.

The third distinct approach to the stopping power problem is the scattering theory formulation [10]. It improves upon quadratic response theory by treating the screening of the projectile to all orders in Z. In the frame of reference of the ion, the electrons in the medium stream by and scatter from a fixed potential, and the net momentum transferred to the projectile is the source of the retarding force. Of course, to implement this approach requires some knowledge of the scattering potential. In the limit of low velocities ($v \ll v_F$) where the stopping power is linear in v, one can obtain the scattering potential by performing a nonlinear screening calculation within density functional theory [11] for a stationary point charge. The angular distortion of the electronic screening cloud around the ion can be neglected in this limit since it leads to corrections which are higher order in v. Previous applications of the method to channelling particles have been quite successful [12] in accounting for both the absolute magnitude of the stopping power and the observed Z-oscillations. Our objective in this paper is to extend these calculations to higher velocities where the screening charge and scattering potential deviate from their form in the low velocity limit. An application to the stopping of antiprotons illustrates our general calculational approach. Interestingly, the linear dependence on v persists in this case up to velocities approaching the stopping power maximum.

2. Theory

Recently, Bönig and Schönhammer [13] have considered the time-dependent problem of an external potential moving with a velocity v through a noninteracting electron gas of density n_0. For a spherically symmetric scattering potential, they arrive at the following expression for the stopping power,

$$S = 2\int \frac{d^3p}{(2\pi\hbar)^3} f(\varepsilon_{p+mv}) \frac{p}{m} p \cdot \hat{v} \sigma_{tr}(p). \tag{1}$$

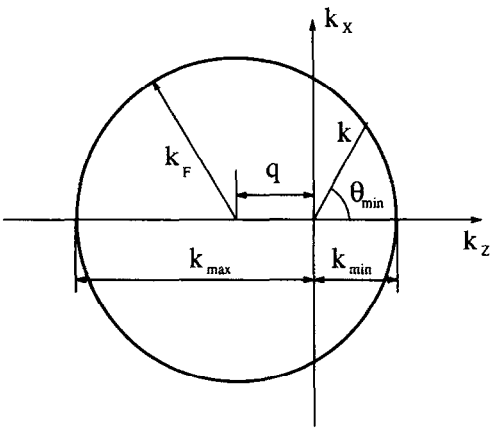

Fig. 1. Schematic of the shifted Fermi sphere and relevant parameters. All states within k_F of the center of the sphere are occupied.

Here $f(\varepsilon_{p+mv})$ is a shifted Fermi distribution at zero temperature, representing the momentum distribution of the electron gas in the projectile frame of reference. In wave vector space, the Fermi sphere is shifted by an amount $q = mv/\hbar$. The factor of 2 accounts for spin degeneracy and $\hat{v}$ is a unit vector in the direction of the moving charge. The momentum transfer (or transport) cross section $\sigma_{tr}(p)$ is defined in terms of the differential scattering cross section $\sigma(\theta, p)$ by

$$\sigma_{tr}(p) = \int d\Omega (1 - \cos\theta) \sigma(\theta, p). \tag{2}$$

By making use of the geometry in Fig. 1 and the kinematic variables defined therein, Eq. (1) can be expressed as

$$S = \frac{\hbar^2}{4\pi^2 m} \int_{k_{min}}^{k_{max}} dk\, k^4 \left[1 - \cos^2\theta_{min}(k)\right] \sigma_{tr}(k). \tag{3}$$

In the low velocity limit, Eq. (3) reduces to the familiar expression [10]

$$S \simeq m v_F v n_0 \sigma_{tr}(k_F), \tag{4}$$

in which the transport cross section is evaluated at the Fermi momentum k_F. If the scattering phase shifts $\delta_l(k)$ are available for the given scattering potential, the momentum transfer cross section can be conveniently evaluated using [14]

$$\sigma_{tr}(k) = \frac{4\pi}{k^2} \sum_{l=0}^{\infty} (l+1) \sin^2(\delta_{l+1} - \delta_l). \tag{5}$$

In both their original [13] and subsequent [15] work, Bönig and Schönhammer studied the scattering of electrons from a hard sphere potential. Here we take the additional step of determining the scattering potential self-consistently. For a charged projectile, each electronic scattering state contributes to the screening of the projectile's bare Coulomb potential, and as a result, the effective scattering potential is itself dependent on the form of the

electronic states. To close this loop we make use of density functional theory [16] which requires the self-consistent solution of the equations (we use atomic units henceforth, $e = m = \hbar = 1$)

$$V(r) = -\frac{Z}{r} + \phi(r) + v_{xc}(r), \tag{6}$$

$$\phi(r) = \int d^3r' \frac{\delta n(r')}{|r - r'|}, \tag{7}$$

$$n(r) = 2 \sum_{k(occ)} |\psi_k(r)|^2, \tag{8}$$

where the single-particle states $\psi_k(r)$ are obtained from the solution of the Schrödinger equation

$$\left[-\tfrac{1}{2}\nabla^2 + V(r)\right]\psi_k(r) = \tfrac{1}{2}k^2\psi_k(r). \tag{9}$$

The effective scattering potential $V(r)$ consists of the external Coulomb potential of the projectile, the electrostatic potential $\phi(r)$ of the screening charge density $\delta n(r) = n(r) - n_0$, and the exchange-correlation potential $v_{xc}(r)$. Since the electrons are streaming past the projectile, the set of occupied states in the k-summation extends over a shifted Fermi sphere. As a result, $n(r)$ and $V(r)$ have axial symmetry only, in contrast to the static screening situation, and the usual procedures for solving the Schrödinger equation for spherical potentials are inapplicable. An expansion of $\psi_k(r)$ in spherical harmonics would lead to a set of coupled radial equations for the angular momentum components and would necessitate a coupled-channels technique for their solution. To avoid this complexity we have adopted the simplest reasonable approximation of replacing $V(r)$ by a spherically symmetric potential to be defined. In this case the scattering states with outgoing wave boundary conditions have the usual form

$$\psi_k(r) = \sum_{lm} 4\pi i^l e^{i\delta_l} Y^*_{lm}(\hat{k}) R_{kl}(r) Y_{lm}(\hat{r}), \tag{10}$$

where the radial wave function R_{kl} is the regular solution of the radial Schrödinger equation. With these solutions the spherically averaged screening density is given by

$$\begin{aligned}\bar{n}(r) &= 2 \sum_{k(occ)} \sum_{l} (2l+1) R^2_{kl}(r) \\ &= \sum_l (2l+1)\left[\frac{1}{\pi^2}\int_0^{k_{min}} dk\, k^2 R^2_{kl}(r) \right. \\ &\quad \left. + \frac{1}{2\pi^2}\int_{k_{min}}^{k_{max}} dk\, k^2 [1 - \cos\theta_{min}(k)] R^2_{kl}(r)\right].\end{aligned} \tag{11}$$

This density is then used to define a spherically symmetric potential $\bar{V}(r)$ according to Eq. (6) which we use in the solution of Eq. (9). This is the main approximation used in our work. While the kinematical effects are explicitly included through the occupancy of the electronic states, the modification of the scattering potential is only included in an average way.

Apart from the shifted Fermi sphere, the numerical procedures used to achieve self-consistency are the same as for the static case [11]. Once the equations have been iterated to convergence, the final spherical potential is used to determine the scattering phase shifts, the scattering cross section and the stopping power. Despite the assumed spherical symmetry of the scattering potential, the density itself is not spherically symmetric due to the summation over the shifted Fermi sphere. It has the form

$$n(r, \theta) = n_1(r) + n_2(r, \theta) \tag{12}$$

where the spherically symmetric component is given by

$$n_1(r) = \frac{1}{\pi^2}\sum_l (2l+1)\int_0^{k_{min}} dk\, k^2 R^2_{kl}(r). \tag{13}$$

This contribution arises only for $q < k_F$ (see Fig. 1), otherwise it is zero. The nonspherical component takes a simple form along the projectile axis. In the forward direction,

$$\begin{aligned} n_2(r, \theta = 0) &= \sum_{ll'} \frac{1}{2\pi^2}\int_{k_{min}}^{k_{max}} dk\, k^2 C_{ll'}(k) R_{kl}(r) R_{kl'}(r) \\ &\equiv \sum_{ll'} n_{ll'}(r) \end{aligned} \tag{14}$$

where

$$\begin{aligned} C_{ll'}(k) &= (2l+1)(2l'+1)\int_0^{\theta_{min}(k)} \sin\theta P_l(\cos\theta) \\ &\qquad \times P_{l'}(\cos\theta)\, d\theta \\ &\times \begin{cases} (-1)^{(l-l')/2}\cos(\delta_l - \delta_{l'}), & \text{if } (l-l') \text{ is even} \\ (-1)^{(l'-l+1)/2}\sin(\delta_l - \delta_{l'}), & \text{if } (l-l') \text{ is odd.} \end{cases} \end{aligned} \tag{15}$$

This coefficient is symmetric in the indices l and l'. Behind the projectile, we have

$$n_2(r, \theta = \pi) = \sum_{ll'} (-1)^{l+l'} n_{ll'}(r). \tag{16}$$

For points off the projectile axis the expression for $n_2(r, \theta)$ takes a slightly more complex form which we do not display here as we shall restrict our calculations of the induced density to the projectile axis.

3. Results and discussion

As an application of the above results we consider the situation of an antiproton moving through an electron gas

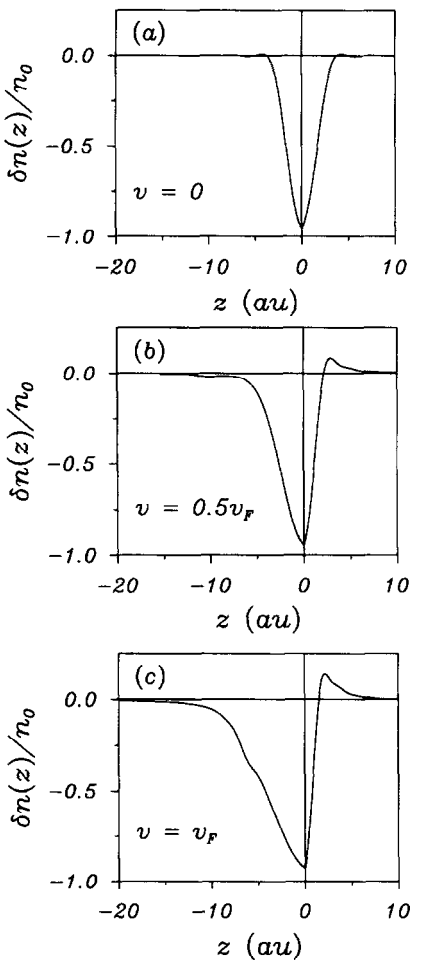

Fig. 2. Normalized screening charge densities along the axis of motion of the antiproton for various velocities: (a) $v = 0$, (b) $v = 0.5v_F$, and (c) $v = v_F$.

corresponding to aluminium densities ($r_s = 2.07$; $v_F = 0.927$ a.u.). Previously, we considered this situation in the low velocity limit in a study of the differences between the stopping characteristics of protons and antiprotons [17]. Fig. 2 shows the axial charge density for a sequence of projectile velocities up to $v = v_F$. Beyond this point the results become sensitive to the radial extent used in the numerical calculations and the number of partial waves used in the construction of the screening density. In addition, it is difficult to obtain a well-converged self-consistent solution. All of these problems are associated with the increasing radial extent and asymmetry of the screening charge as displayed in Fig. 2. Of course, our neglect of the asymmetry in the scattering potential is less justifiable at the higher velocities, and quite apart from the numerical difficulties, we believe that our results would not be very meaningful beyond about $v = v_F$.

At $v = 0$, the axial density shown is the same as that found previously [17] and displays the pronounced depletion hole induced by the negatively charged antiproton. At finite projectile velocities, however, a marked asymmetry in the depletion hole develops with increasing velocity. In the forward direction (positive z values), the induced density increases above its value in the $v = 0$ limit, indicating that the electrons are able to penetrate closer to the negatively charged antiproton due to their larger relative velocity. As a result, there is a slight increase in the density at the antiproton, $n(0)$, with increasing velocity. Furthermore, there is a region in front of the projectile in which the density accumulates to a value above the ambient electron gas density. This compression of the electron gas is also seen [15] in the motion of an impenetrable object through a compressible fluid. Behind the projectile there is a relative decrease in the electron density which, by $v = v_F$, extends out to 10 a.u. from the projectile. This region of rarefaction, also seen in the hard sphere calculations [15], constitutes the trailing wake in the case of the antiproton. The structure apparent in the trailing density at $v = v_F$ should not be taken too seriously since our use of the spherically averaged potential is no doubt becoming less reliable. Nevertheless, we believe the qualitative behaviour shown in these figures is a good indication of the behaviour to be expected in a more complete calculation.

It is also useful to consider the total integrated charge density within a sphere of radius r:

$$Q(r) = 4\pi \int_0^r \mathrm{d}r'\, r'^2 \delta\bar{n}(r'), \tag{17}$$

where $\delta\bar{n}(r)$ is the deviation of the spherically averaged density defined in Eq. (11) from n_0. Fig. 3 shows $Q(r)$ for $v = 0$, $v = 0.5v_F$ and $v = v_F$. The rate at which $Q(r)$ reaches its limiting value of -1 decreases with increasing velocity, indicating that the screening charge density is becoming more extended. We also note that the total screening charge density preserves overall charge neutrality, consistent with the Friedel sum rule in the static limit,

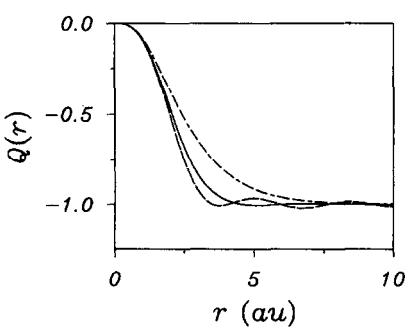

Fig. 3. Integrated screening charge densities, Eq. (17), as a function of the radial distance from the antiproton: $v = 0$ (dashed line), $v = 0.5v_F$ (solid line), $v = v_F$ (dot-dashed line).

and ensuring that the electric fields decay at least as r^{-3} for large distances from the antiproton.

It is instructive at this point to make a comparison of our results with those obtained using linear response theory at the level of the random phase approximation (RPA) [1]. The induced density in RPA is strictly proportional to Z and therefore, apart from an overall sign, has the same form for both protons and antiprotons. In Fig. 4 we show the RPA density for $v = 0.01\ v_F$, $v = 0.5 v_F$, $v = v_F$ and $v = 1.5 v_F$. The lowest velocity is close to the static limit, and is qualitatively similar to the DFT result. However, the density at the antiproton is depleted by about three times the background density which is obviously inconsistent with the requirement that $|\delta n(0)/n_0| \leq 1$. The fact that the magnitude of the RPA density is exaggerated near the antiproton implies that the external charge is screened within a smaller distance than is possible in the DFT calculation. This is particularly evident at the higher velocity of $v = v_F$ which shows the density falling off within about 5 a.u. on the trailing side of the antiproton, approximately half the extent of the trailing wake in the DFT calculation. In Fig. 4 we also show the density for $v = 1.5 v_F$ which is well into the regime of collective plasmon wake formation. An even more dramatic view of the plasmon wake is provided by the plots of $Q(r)$ in Fig. 5 which show the large increase in the oscillation amplitude on going from $v = v_F$ to $v = 1.5 v_F$. A comparison with Fig. 3 for $v = v_F$ shows that the oscillation amplitude is much smaller in the DFT calculation, although it should be borne in mind that the latter makes use of the spherical potential approximation while the RPA does not.

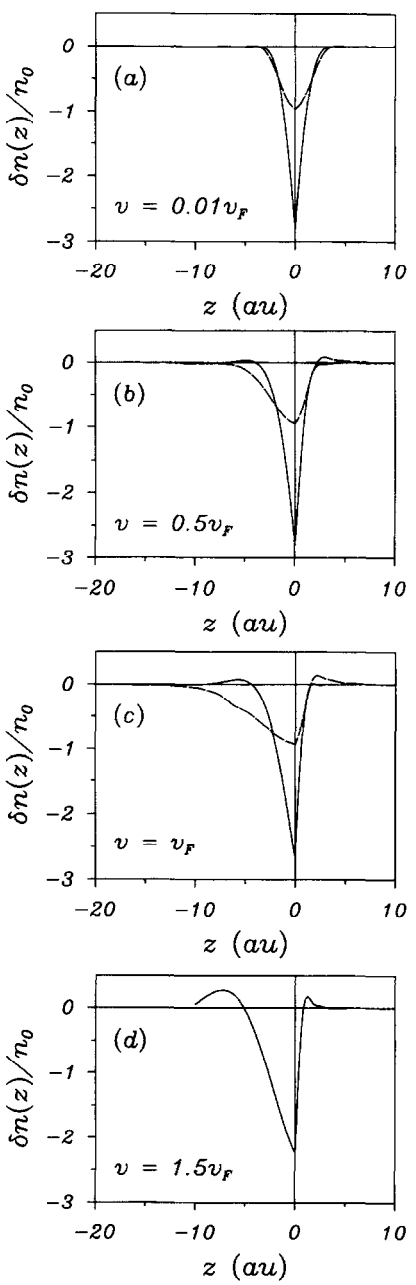

Fig. 4. Normalized screening charge densities along the axis of motion of the antiproton as calculated in linear response theory (solid lines). The corresponding nonlinear densities are shown as dashed lines.

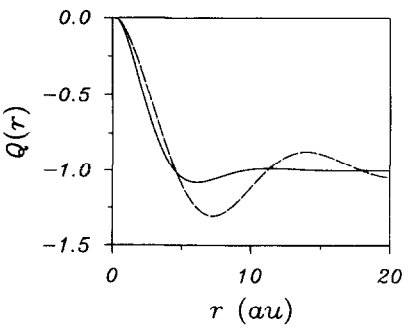

Fig. 5. Integrated screening charge densities as a function of the radial distance from the antiproton, as calculated in linear response theory: $v = v_F$ (solid line), $v = 1.5 v_F$ (dashed line).

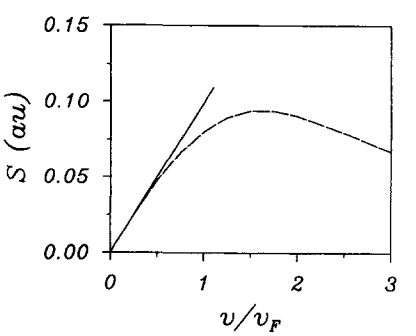

Fig. 6. Antiproton stopping power as a function of velocity (solid curve). The dashed curve is obtained using the statically screened ($v = 0$) potential.

Fig. 6 shows the stopping power as a function of velocity. It is noteworthy that the stopping power depends almost linearly on v up to $v = v_F$ and thus provides a theoretical explanation for the empirical conclusions arrived at by Mann and Brandt [3] on the basis of a survey of stopping power data. The near-perfect linearity is a consequence of two competing effects. The first is the effect of the shifting Fermi sphere. Fig. 6 shows the result obtained if the static ($v = 0$) scattering potential is used to obtain the cross section. The negative curvature is a phase space effect associated with the different sampling of the scattering cross section, while the decrease seen at high velocities can be understood in terms of a diminishing cross section with increasing kinetic energy. The second effect is the modification of the scattering potential with increasing velocity. The average dynamically screened potential is stronger than the static potential and the cross section for it is correspondingly larger. This compensates for the phase space effect and straightens out the stopping power curve. It would be of interest to extend these results to the stopping power maximum and beyond, but as mentioned previously, it would not be meaningful to do so within the present approximation scheme. If the calculations could be done, it would be particularly interesting to see whether the sudden increase in stopping power found in both the linear [18] and quadratic [9] response theories at the onset of collective excitations survives in the fully nonlinear calculation.

We should at this point explain why we expect collective effects to show up in our calculations of the screening charge even though they appear to be based on a single-particle picture. To clarify this point, we note that the linear density response function for a noninteracting electron gas occupying a shifted Fermi sphere, $\chi_v^0(q, \omega)$, is given by

$$\chi_v^0(q, \omega) = \chi_{v=0}^0(q, \omega + q \cdot v), \tag{18}$$

i.e. the effect of the shifted Fermi sphere is equivalent to a shift of the frequency in the usual equilibrium response function. Thus in the static limit, we have

$$\chi_v^0(q, 0) = \chi_{v=0}^0(q, q \cdot v). \tag{19}$$

In other words, the static screening for a shifted Fermi sphere is in fact related to the usual density response function at the finite frequency, $\omega = q \cdot v$. The same argument applied to the interacting electron gas shows that the RPA response function is given by

$$\chi_v(q, 0) = \chi_{v=0}(q, q \cdot v). \tag{20}$$

This implies that the dynamic screening charge can be equally well determined by treating the external projectile potential as static, but with the response of the electron gas represented by the response function in Eq. (20). If $q \cdot v$ intersects the plasmon branch, as it must at sufficiently large v, the induced screening charge will obviously acquire a collective contribution. The spirit of the DFT calculation is the same as a calculation based on Eq. (20) in the sense that the static projectile potential is screened by a moving electron gas, with the only difference being that the response is determined nonlinearly. We suspect that at least some of the numerical difficulties encountered above $v = v_F$ are associated with the onset of collective excitations which has the effect of making the scattering potential much more extended in space.

4. Conclusions

To conclude, we have shown that it is possible to extend the low velocity stopping power calculations to finite projectile velocities by allowing the electrons to occupy a shifted Fermi sphere. Our results for antiprotons for velocities less than v_F demonstrate that, within the spherical potential approximation, the stopping power is a linear function of the projectile velocity. At the higher velocities where an extended collective wake is expected to form, the nonsphericity of the scattering potential is becoming increasingly important, and a refined couple-channels calculation is needed. The application to positively charged projectiles which support bound states would also be of interest. However, such a calculation is much more complex since it requires a prescription for the capture and loss processes which determine the occupancy of the available bound states [19]. These, and other extensions, are interesting projects for future consideration.

Acknowledgement

This work was supported by grants from the Natural Sciences and Engineering Research Council of Canada, the Comision Asesora de Investigación Científica y Técnica and the Department of Education of the Basque Government.

References

[1] J. Neufeld and R.H. Ritchie, Phys. Rev. 98 (1955) 1632;
V.N. Neelavathi, R.H. Ritchie and W. Brandt, Phys. Rev. Lett. 33 (1974) 302; ibid. 33, 670 (E) (1974);
P.M. Echenique, R.H. Ritchie and W. Brandt, Phys. Rev. B 20 (1979) 2567;
A. Mazarro, P.M. Echenique and R.H. Ritchie, Phys. Rev. B 27 (1983) 4117.

[2] J. Lindhard, K. Dan. Vidensk. Selsk. Mat.-Fys. Medd. 28 (8) (1954).

[3] A. Mann and W. Brandt, Phys. Rev. B 24 (1981) 4999;
P.M. Echenique, R.M. Nieminen and R.H. Ritchie, Solid State Commun. 37 (1981) 779.

[4] F. Bloch, Z. Phys. 81 (1933) 363;
R. Kronig and J. Korringa, Physica 10 (1955) 406;

S. Lundqvist, in: Theory of the Inhomogeneous Electron Gas, eds. S. Lundqvist and N.H. March (Plenum, New York, 1983) p. 149.

[5] L.H. Thomas, Proc. Camb. Philos. Soc. 23 (1926) 542;
E. Fermi, Z. Phys. 48 (1928) 73;
C.F. von Weizsäcker, Z. Phys. 96 (1935) 431.

[6] A. Arnau and E. Zaremba, Nucl. Instr. and Meth. B 90 (1994) 32;
J.J. Dorado, O.H. Crawford and F. Flores, Nucl. Instr. and Meth. B 93 (1994) 175, and erratum 95 (1995) 144.

[7] C.D. Hu and E. Zaremba, Phys. Rev. B 37 (1988) 9268.

[8] C.C. Sung and R.H. Ritchie, Phys. Rev. A 28 (1983) 674;
H. Esbensen and P. Sigmund, Ann. Phys. (New York) 201 (1990) 152.

[9] J.M. Pitarke, R.H. Ritchie and P.M. Echenique, Nucl. Instr. and Meth. B 79 (1993) 209;
J.M. Pitarke, R.H. Ritchie, P.M. Echenique and E. Zaremba, Europhys. Lett. 24 (1993) 613.

[10] B.A. Trubnikov and Yu. N. Yavlinskii, Sov. Phys. JETP 21 (1965) 167;
E. Bonderup, Penetration of Charged Particles Through Matter (Lecture notes, University of Aarhus, 1981);
P.M. Echenique, I. Nagy and A. Arnau, Int. J. Quantum Chem. 23 (1989) 521.

[11] C.O. Almbladh, U. von Barth, Z.D. Popovic and M.J. Stott, Phys. Rev. B 14 (1976) 2250;
E. Zaremba, L.M. Sander, H.B. Shore and J.H. Rose, J. Phys. F7 (1977) 1763.

[12] P.M. Echenique, R.M. Nieminen, J.C. Ashley and R.H. Ritchie, Phys. Rev. A 33 (1986) 897;
I. Nagy, A. Arnau and P.M. Echenique, Phys. Rev. A 40 (1989) 987;
M. Peñalba, A. Arnau and P.M. Echenique, Nucl. Instr. Meth. B 67 (1992) 66.

[13] L.Bönig and K. Schönhammer, Phys. Rev. B 39 (1989) 7413.

[14] C. Kittel, Quantum Theory of Solids (Wiley, New York, 1963).

[15] W. Zwerger, L. Bönig and K. Schönhammer, Phys. Rev. B 43 (1991) 6434.

[16] W. Kohn and P. Vashishta, in Theory of the Inhomogeneous Electron Gas, ed. S. Lundqvist and N.H. March (Plenum, New York, 1983) p. 91.

[17] I. Nagy, A. Arnau, P.M. Echenique and E. Zaremba, Phys. Rev. B 40 (1989) 11983; ibid. B 44 (1991) 12172.

[18] J. Lindhard and A. Winther, K. Dan. Vidensk. Selsk. Mat.-Fys. Medd. 34(4) (1964).

[19] P.M. Echenique, F. Flores and R.H. Ritchie, Dynamic Screening of Ions in Condensed Matter, in Solid State Physics vol. 43, eds. H. Ehrenreich and D. Turnbull (Academic Press, New York, 1990);
A. Arnau, M. Peñalba, P.M. Echenique, F. Flores and R.H. Ritchie, Phys. Rev. Lett. 65 (1990) 1024.